

Temperature- and pressure-induced structural transitions in rare-earth-deficient $R_{1-x}Ni_2$ (R = Y, Sm, Gd, Tb) Laves phases

This article has been downloaded from IOPscience. Please scroll down to see the full text article.

1996 J. Phys.: Condens. Matter 8 8351

(<http://iopscience.iop.org/0953-8984/8/43/026>)

View [the table of contents for this issue](#), or go to the [journal homepage](#) for more

Download details:

IP Address: 171.66.16.207

The article was downloaded on 14/05/2010 at 04:24

Please note that [terms and conditions apply](#).

Temperature- and pressure-induced structural transitions in rare-earth-deficient $R_{1-x}Ni_2$ ($R = Y, Sm, Gd, Tb$) Laves phases

E Gratz^{†*}, A Kottar[†], A Lindbaum[†], M Mantler[‡], M Latroche[§],
V Paul-Boncour[§], M Acet^{||}, C I Barner^{||}, W B Holzapfel[¶], V Pacheco⁺ and
K Yvon⁺

[†] Institute for Experimental Physics, Technical University of Vienna, Wiedner-Hauptstrasse 8-10, A-1040 Wien, Austria

[‡] Institute for Technical and Applied Physics, Technical University of Vienna, Austria

[§] Laboratoire de Chimie Metallurgique des Terres Rares, CNRS Meudon Cédex, France

^{||} Laboratory for Low Temperature Physics, University of Duisburg, Germany

[¶] Fachbereich Physik, University of Paderborn, Germany

⁺ Laboratoire de Cristallographie, University of Geneva, Switzerland.

Received 21 June 1996, in final form 12 August 1996

Abstract. Electrical resistivity, thermal expansion, and temperature-dependent x-ray diffraction measurements on $R_{1-x}Ni_2$ compounds give mutually consistent evidence for structural phase transitions at 740 K, 550 K, 600 K, and 450 K respectively for $R = Y, Sm, Gd, Tb$; $0 < x < 0.05$. Arguments are given as to why most of the rare-earth–nickel compounds with the 1:2 ratio do not crystallize in the simple cubic Laves phase (C15 type) but show a superstructure of the cubic Laves phase at room temperature and at ambient pressure. This superstructure with the space group $F\bar{4}3m$ and a doubled cell parameter is characterized by ordered vacancies on the R sites. It is shown that the observed structural instabilities result in transitions to the cubic Laves phase (space group $Fd\bar{3}m$), however with *disordered* vacancies at high temperatures. High-pressure x-ray powder diffraction experiments show that the phase transition in $Y_{0.95}Ni_2$ shifts down to room temperature for a pressure of 27 GPa.

1. Introduction

It is usually assumed that the $R_{1-x}Ni_2$ compounds crystallize in the cubic Laves phase structure type C15 [1]. This structure type exists [2] when the composition is near $x = 0.007$. However, the existence of structural defects has been reported for several RNi_2 compounds, such as $LaNi_2$ and $CeNi_2$ [3, 4]. Furthermore, the existence of structural defects has been discussed also for the case of $TmNi_2$ [5].

First attempts to determine the distribution of defects for $R_{1-x}Ni_2$ have been made using x-ray and neutron powder diffraction [6, 7], with the main conclusion that the $R_{1-x}Ni_2$ compounds crystallize in a superstructure of the cubic Laves phase (space group $F\bar{4}3m$) with regular R vacancies and a doubled lattice parameter. In a previous investigation of the transport properties (electrical resistivity, thermal conductivity, and thermopower) of the RNi_2 series, discontinuities were observed in some of these compounds at high temperatures [8]. A similar observation in resistivity measurements has been made for YNi_2 [9] referring

* Author to whom any correspondence should be addressed.

the anomaly to an onset of a tetragonal distortion of the cubic Laves phase. In further attempts to explain these anomalies in terms of a structural phase transition [10] no detailed explanation for the type of transition could be given at that time. The main problem (as we know now) was the oxidation of the powdered samples during the high-temperature x-ray experiments.

The present paper adds now some new results on high-temperature transport phenomena (electrical resistivity), single-crystal x-ray diffraction at room temperature, high-temperature x-ray powder diffraction under improved conditions, x-ray powder diffraction under pressure (using synchrotron radiation) and thermal expansion measurements in the vicinity of the corresponding transitions. The high-temperature phases and the structural instabilities in RNi_2 compounds with $R = Y, Sm, Gd,$ and Tb , have been studied.

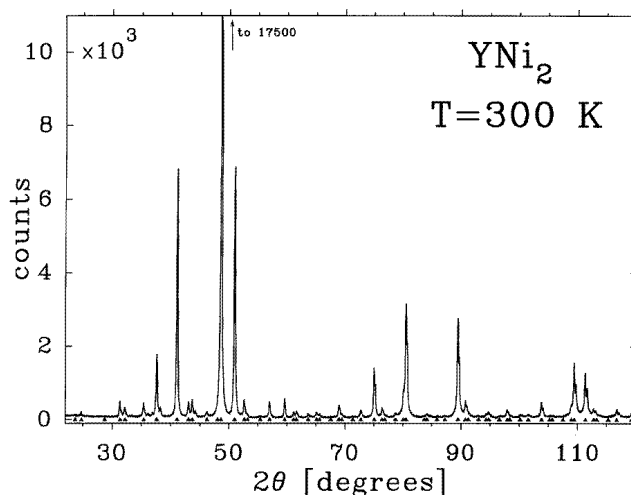


Figure 1. A typical x-ray diffraction pattern for the superstructure of the cubic Laves phase (space group $F\bar{4}3m$) characterized by a doubling of the lattice parameter and by the existence of regular vacancies. This pattern was measured at room temperature for the case of YNi_2 using $Co K\alpha$ radiation. The lattice parameter $a = 14.35 \text{ \AA}$.

2. Experimental details

The first step from an experimental point of view was the preparation of single-phase samples for those RNi_2 compounds ($R = Y, Sm, Gd$) where the transition has been observed earlier. During the present investigation it was noticed that this phase transition exists also in one neighbouring compound of $GdNi_2$, namely in $TbNi_2$. The effort to work with pure single-phase samples was necessary to exclude effects from impurity phases as possible reasons for the observed phase transitions. For example, samples with $x > 0.05$ ($R_{1-x}Ni_2$) frequently show the (hexagonal) RNi_3 phase as an impurity, whereas samples with the exact 1:2 stoichiometry show the RNi phase (tetragonal, CrB structure type) in a small quantity depending on the heat treatment.

All of the samples showed superstructure with the space group $F\bar{4}3m$. In figure 1 the room temperature x-ray pattern of the Y compound with the stoichiometry 0.95:2 (on which all the experiments have been done) is depicted. (Note that for simplicity we are

still using RNi_2 to indicate the compounds under consideration.) The marks in this figure correspond to the superstructure (space group: $F\bar{4}3m$) with the doubled unit-cell parameter of the cubic Laves phase (space group: $Fd\bar{3}m$). The phase purity was checked additionally by a metallographic method.

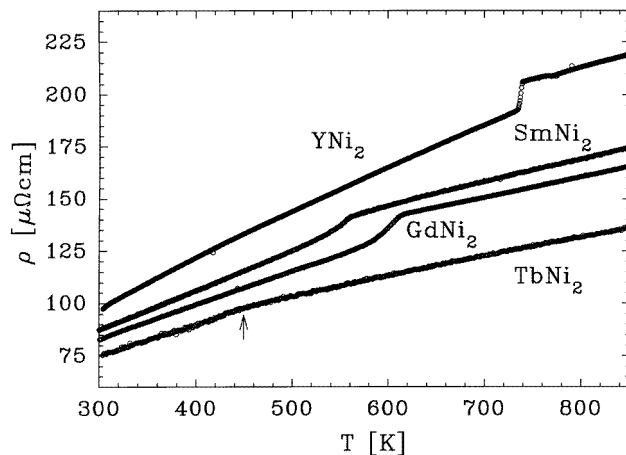


Figure 2. The temperature dependence of the electrical resistivity of YNi_2 , $SmNi_2$, $GdNi_2$ and $TbNi_2$ is shown in the temperature range above room temperature. The discontinuities in ρ versus T mark the corresponding phase transitions (the arrow indicates the transition of $TbNi_2$). These ρ versus T curves are obtained with increasing temperatures.

The resistivity experiments, which turned out to give very sensitive indications for the phase transitions, were performed in the temperature range from 4.2 K up to 1000 K. The x-ray diffraction above room temperature used a high-temperature chamber (built by the A Paar Company, Austria) on a Siemens D5000 powder diffractometer with $Cu\ K\alpha$ radiation. To prevent oxidation during measurements in the temperature range far above room temperature, the vacuum inside the chamber was kept at 10^{-6} mbar. Thermal expansion measurements were done on YNi_2 , $SmNi_2$ and $GdNi_2$ in two capacitive dilatometers, covering the temperature ranges 4 K to 300 K and 300 K to 1200 K. Additionally high-pressure x-ray diffraction experiments have been carried out on YNi_2 . The high-pressure x-ray diffraction experiments were performed with synchrotron radiation in HASYLAB at DESY in the energy-dispersive mode using a diamond-anvil cell to generate pressures in the range up to 30 GPa [11] with the use of ruby fluorescence for the pressure measurement [12, 13]. Density measurements have been made for YNi_2 using an Accupyc 1330 Micromeritics pycnometer. On this sample we also performed DTA measurements on a SETARAM 92-16 apparatus. We finally completed our experimental investigations by a detailed study of a small single crystal of YNi_2 at room temperature. This single-crystal investigation on YNi_2 was performed on an automated four-circle x-ray diffractometer by collecting 5410 reflections at room temperature, yielding a set of 170 symmetry-independent intensities of which 100 can be classified as superstructure intensities resulting from the doubling of the C15 type cell. The refined cell parameter, $a = 14.377(2)$ Å, is somewhat larger and more precise than the one reported from powder diffraction in [6] ($a = 14.350(4)$ Å). The atomic positions, occupancies, and displacements were refined according to a structure proposed in [6] with space group $F\bar{4}3m$, and five Y sites, four Ni sites; however, the atomic displacement parameters were all allowed to vary independently in the present work.

3. Results and discussion

3.1. Electrical resistivity

Figure 2 shows the temperature variation of the electrical resistivity ρ of YNi_2 , SmNi_2 , GdNi_2 and TbNi_2 in the region above room temperature. These curves exhibit anomalies in ρ versus T near to the following temperatures: 740 K (YNi_2), 550 K (SmNi_2), 600 K (GdNi_2), and 430 K (TbNi_2). These anomalies in YNi_2 and GdNi_2 are found roughly at the same temperatures as previously [10]. In the case of SmNi_2 the corresponding anomaly was previously thought to occur roughly at 920 K and the much smaller anomaly around 550 K was overlooked. TbNi_2 had not been studied from this point of view previously.

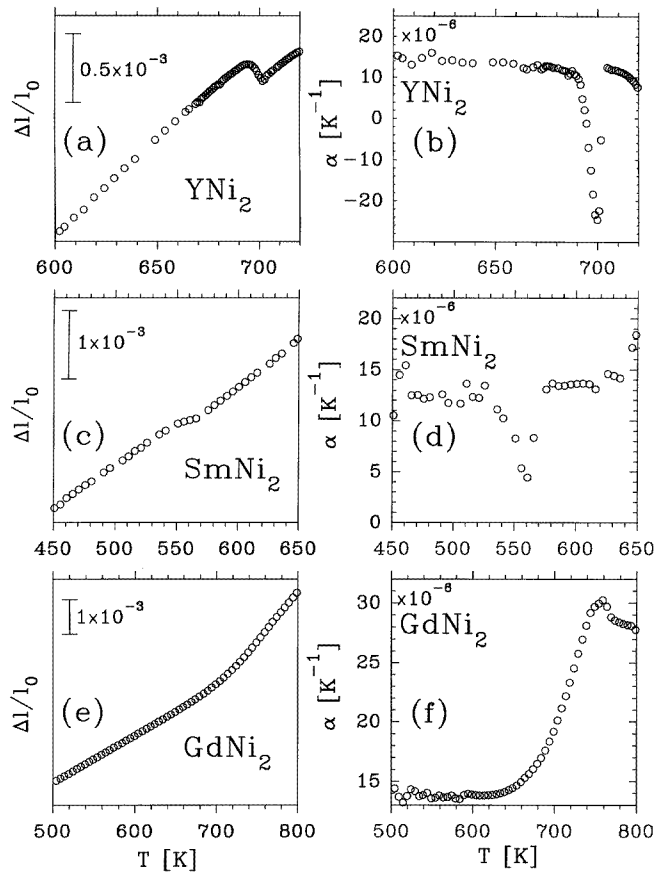


Figure 3. The thermal expansion $\Delta l/l_0$ and the coefficient of the thermal expansion α in the vicinity of the corresponding transition temperatures are shown for YNi_2 ((a) and (b)), for SmNi_2 ((c) and (d)) and for GdNi_2 ((e) and (f)).

The ρ versus T curves shown in figure 2 are obtained with increasing temperature. In all of these cases hysteresis effects exist at the transition. Beside the step-like anomaly in ρ versus T , the slope ($d\rho/dT$) below the transition is larger than that above. Since $d\rho/dT$ in the high-temperature region is determined by the electron-phonon scattering, the change in slope is related to the change in the phonon spectra above the transition. According

to the Bloch–Grüneisen relation, which describes the electron–phonon interaction and its influence on the temperature variation of the resistivity (see, e.g., [14]), we conclude that the Debye temperature of the high-temperature phase is higher (it follows from the smaller value of $d\rho/dT$) than that of the superstructure below the transition. That means that the lattice with nonlocalized vacancies is stiffer (more dense) in agreement with the thermal expansion measurements (see below).

3.2. Thermal expansion

Any volume change associated with a structural transition is detected very sensitively in thermal expansion measurements. Therefore, we have measured the (linear) thermal expansion as a function of temperature for the three samples YNi_2 , $SmNi_2$, and $GdNi_2$. Figure 3 shows the curves for $\Delta l/l_0$ versus T and the coefficient α versus T in the vicinity of the transitions, for the Y compound (figures 3(a) and 3(b)), for the Sm compound (figures 3(c) and 3(d)) and for the Gd compound (figures 3(e) and 3(f)). As can be seen, there is indeed a shrinking of the volume by about 1×10^{-4} (see figures 3(a) and 3(c)). For YNi_2 and $SmNi_2$ a decrease in $\Delta l/l_0$ is observed at temperatures very near to the step-like anomaly in the resistivity. In $GdNi_2$, the transition takes place over a broader temperature range and is qualitatively different in comparison to those for the other two compounds. This is not yet understood. $TbNi_2$ has not been investigated with respect to the thermal expansion.

Since these transitions occur in the nonmagnetic YNi_2 compound and far above the magnetic ordering temperatures of any of the magnetic RNi_2 compounds ($SmNi_2$: $T_C = 21$ K; $GdNi_2$: $T_C = 80$ K; and $TbNi_2$: $T_C = 40$ K), these structural transitions are obviously not of magnetic origin. Because these anomalies exist in sample materials independently of whether there are small quantities of foreign phases (see below), we may assume that this transition is an intrinsic property of these RNi_2 compounds and not caused by impurities. The possible dependence of the transitions on the amounts of foreign phases has been checked in the case of $Y_{1-x}Ni_2$ by preparing samples with different values of x ($x < 0.05$). Independently of the amount and structure of the impurity phase, the transition under consideration *exists* in all of these Y-based samples and the same observation was made for the other compounds. However, the width of the hystereses at the transitions is influenced by the amount of the impurity phase.

3.3. Differential thermal analysis

From the DTA curve, it is observed that the transition is reversible and endothermic upon heating, which is characteristic of an order–disorder transition. From the integration of the peak at the transition in case of YNi_2 , we estimated the enthalpy as 1.35 J g^{-1} which is a very low value according to the fact that the transition is related to 5% vacancy ordering.

3.4. X-ray diffraction

3.4.1. X-ray powder diffraction at high temperature. For the determination of the nature of this structural transition we used, as in the previous investigation [10], high-temperature x-ray diffraction measurements. In figures 4(a) and 4(b) the x-ray pattern of YNi_2 at 670 K (below the transition) and 850 K (above the transition) are shown as examples. As one can see the superstructure lines present at 670 K in figure 4(a) disappear above the transition, i.e. the pattern at 850 K (figure 4(b)) corresponds to the known cubic Laves phase. In agreement with the reversibility of this transition, observed in resistivity and

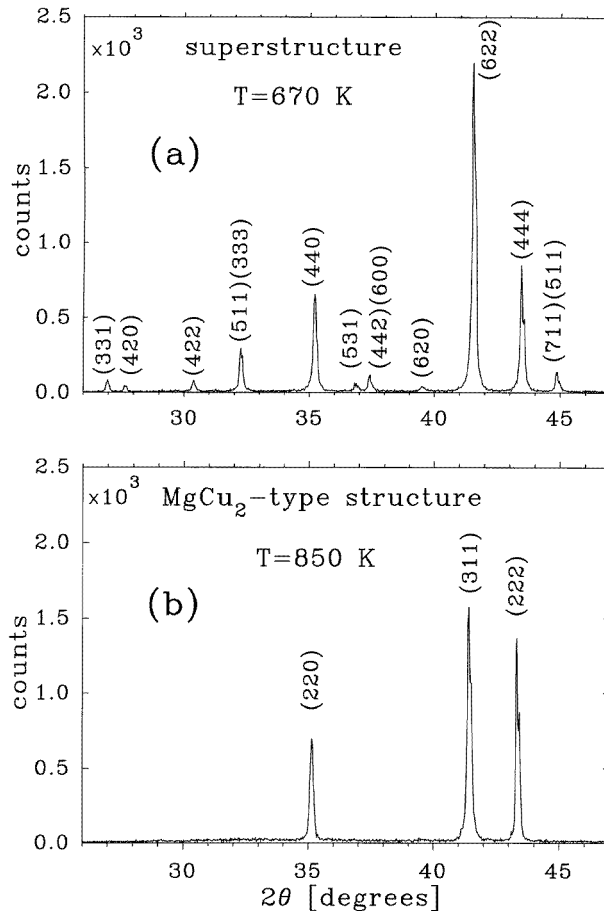


Figure 4. The x-ray pattern of YNi_2 obtained using $\text{Cu K}\alpha$ radiation. (a) Below the transition (670 K), the indices correspond to the superstructure with the space group $F\bar{4}3m$. (b) Above the transition (850 K), the indices correspond to the MgCu_2 structure with the space group $Fd\bar{3}m$.

thermal expansion measurements, the superstructure lines are obtained again after cooling the sample below about 700 K. The high-temperature x-ray measurements performed on Gd, Sm, and Tb samples show the same behaviour as the Y compound.

After we had clarified the nature of the transition, the question concerning the reason for this instability arose immediately. However, at first it appears to be necessary to concentrate on the question of why the RNi_2 compounds at least with the elements Y, Sm, Gd, and Tb do not crystallize in the MgCu_2 -type structure at room temperature. In preparing RT_2 ($T = \text{Mn, Fe, Co and Ni}$) Laves phase samples with the 1:2 stoichiometry, we made the general observation that it becomes progressively more difficult to obtain single-phase samples, when starting with the heaviest R elements and proceeding towards the light R elements. Even a very long annealing procedure does not give in many cases pure Laves phase samples.

One well known case is that of the YCo_2 compound. In that case the impurity phase is especially disturbing because the YCo_3 impurity phase is ferromagnetic, and therefore

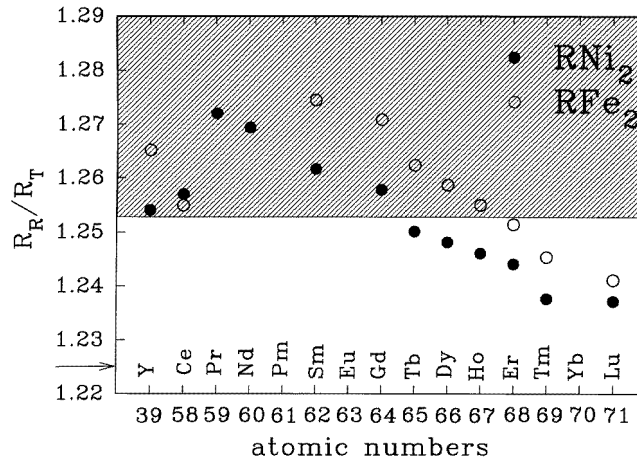


Figure 5. The atomic radius ratios, R_R/R_T with the rare-earth radius determined from the lattice constant ($R_R = a(3/8)^{1/2}$) and the R_T -values for Ni (1.24 Å) and Fe (1.26 Å) considered as constants for this series. Note, the lanthanide contraction with increasing atomic number is clearly visible.

prevents magnetic studies of the paramagnetic YCo_2 compound [15].

To explain this observation it is interesting to consider R_R/R_T , the ratio of the rare-earth and the transition metal atomic radii which these elements take in the Laves phase structure. In figure 5 this ratio for the two series RFe_2 and RNi_2 is shown. Note that the most compact arrangement of hard spheres of the two sizes within the unit cell is obtained for $R_R/R_T = 1.225$. As can be seen from figure 5 the deviation from this ideal value is remarkable even for the Lu compounds and increases further toward the light-R-element compounds for both series. Experimentally we observed that there is some kind of a threshold indicated by the line ($R_R/R_T \approx 1.25$) in figure 5, where the preparation of a Laves phase compound is hardly possible (hatched area). Just as an example, it was not possible to prepare $PrFe_2$ and $NdFe_2$ as single-phase samples (at least we did not succeed under normal conditions, i.e. without applying pressure).

Coming back to the RNi_2 , we obtained single-phase samples for compounds with a ratio R_R/R_T near to this threshold of about 1.25, however, showing the superstructure for these RNi_2 compounds.

As already mentioned above and discussed in more detail below, this superstructure is characterized by regular vacancies on the R sites. This is an interesting fact since it enables us to give at least a qualitative explanation of why the superstructure appears in these four compounds with such an enhanced ratio R_R/R_T . Due to the increasing R atomic radius towards the light R elements (lanthanide expansion) which directly can be seen in the ratio R_R/R_T , the available space for the transition metal tetrahedra becomes obviously too large in the Laves phase; however, due to the unoccupied R sites the space for these tetrahedra is sufficiently reduced to stabilize a structure very similar to the cubic Laves phase, namely the superstructure. An interesting problem for future investigations is whether the appearance of the superstructure with vacancies in these RNi_2 compounds is some kind of precursor which indicates already that the following 1:2 compound series in the periodic table (RCu_2) with an even larger ratio R_R/R_T will crystallize in a structure with a lower symmetry (orthorhombic $CeCu_2$ -type structure, space group: $Imma$).

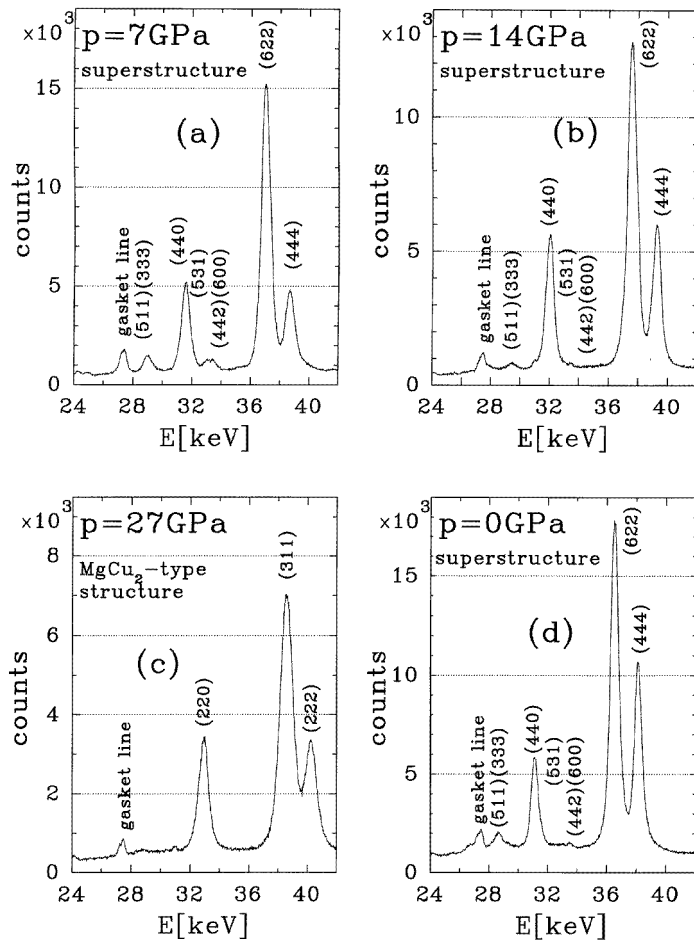
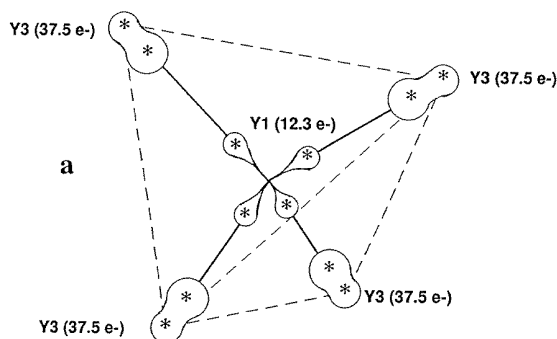


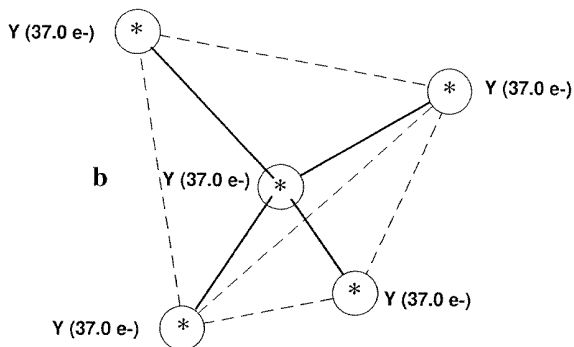
Figure 6. Results for the pressure-induced phase transition in YNi_2 (a) at $p = 7$ GPa and (b) at $p = 14$ GPa (superstructure, space group: $F43m$), (c) at $p = 27$ GPa (MgCu_2 -type structure, space group: $Fd\bar{3}m$), and (d) at $p = 0$ GPa; the superstructure has reappeared after the reduction of the pressure.

3.4.2. X-ray powder diffraction at high pressure. A very rigorous test of such a ‘space-filling’ model is certainly the application of an external pressure—because, if one reduces the available space for the transition metal tetrahedra sufficiently, one should be able to stabilize the cubic Laves phase at room temperature. Indeed the present pressure experiments performed on a YNi_2 sample with single-phase superstructure at room temperature reveal that pressures higher than about 25 GPa suppress the superstructure at room temperature and stabilize the cubic Laves phase. After decreasing the pressure towards ambient pressure, the superstructure lines are revealed again. These experimental results are illustrated by some energy-dispersive x-ray diffraction patterns in figure 6. Figure 6(a) (7 GPa) and figure 6(b) (14 GPa) show patterns of the superstructure, however with decreasing intensity of the extra lines which finally disappear in the MgCu_2 -type structure at 27 GPa (figure 6(c)). After a pressure decrease to ambient pressure (figure 6(d)) the lines of the superstructure reappear.

3.4.3. *Single crystal x-ray diffraction at room temperature.* Even if these structural results from polycrystalline samples explain in principle why a structure with ordered vacancies appears, there were still open problems which we expected to understand better on completing single-crystal investigations, although single crystals of sufficient size and quality are not easy to obtain. The present single-crystal x-ray study on YNi_2 confirms first of all the structural model [6] from powder diffraction, but gives in addition a more detailed picture of the defect distribution.



Electron density around the Yttrium sites in the *superstructure with ordered vacancies*



Electron density around the Yttrium sites in the *Laves phase with disordered vacancies*

Figure 7. A model of the electron density in the low-temperature superstructure phase with partially ordered vacancies (a) and the high-temperature Laves phase with disordered vacancies (b). The numbers indicate the total number of electrons corresponding to the occupancy factor of the various yttrium atom sites (indicated by asterisks) derived from the single-crystal x-ray diffraction data.

The electron density near two Y sites was modelled in the following way: Y1 on site 4a (0, 0, 0; occupancy 0.24) was replaced by a delocalized site 16e (x, x, x ; $x = 0.027(3)$; refined occupancy 3.1 electrons), and Y3 on site 16e (x, x, x ; $x = 0.1000(2)$; occupancy 1) was split in two sites 16e with $x = 0.094(2)$ and $0.117(2)$ and refined occupancies of 21.2 and 16.4 electrons, respectively. The refinement results in relative deviations for the fitted intensities of $R = 0.0066$ and goodness of fit = 2.06 for 170 unique reflections and 20 refined parameters.

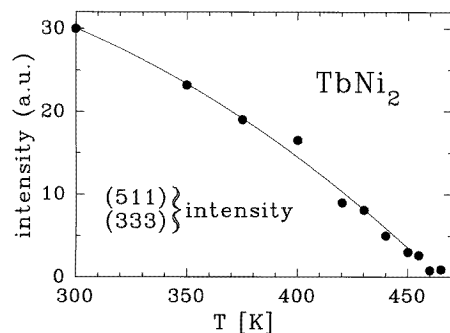


Figure 8. The decrease of the intensity of the (511, 333) superstructure line with temperature for the TbNi_2 compound.

As shown qualitatively in figure 7, the electron density near the Y1 site (point symmetry $\bar{4}3m$) is relatively low and delocalized by about 0.67 \AA on four symmetry-equivalent positions (marked by asterisks) which are occupied by a total number of 12.3 electrons. The electron density near the neighbouring Y3 site (point symmetry $3m$) is relatively high and delocalized on two sites (marked by two asterisks) which are separated by about 0.54 \AA and occupied by 16.4 and 21.1 electrons, respectively, giving a total of 37.5 electrons (Y: 39 electrons). Thus the environment of both Y1 and Y3 is partially disordered at room temperature. Assuming that all delocalized and/or split atom sites are occupied by yttrium only, the calculated composition of the crystal ($\text{Y}_{0.95}\text{Ni}_2$) is consistent with the nominal composition of the sample ($\text{Y}_{0.95}\text{Ni}_2$). However, the calculated density of this model (7.25 g cm^{-3}) is significantly higher than the experimentally measured density ($7.21(1) \text{ g cm}^{-3}$). Assuming that yttrium on these sites is partly substituted for with nickel (which is likely in view of the small separation between certain sites) a better agreement between the experimental and calculated densities (7.20 g cm^{-3}) is obtained, but the composition of such a model ($\text{Y}_{0.88}\text{Ni}_2$) can be considered to be outside the error limit of the stoichiometry. Further experiments are required to solve this problem. From the gradual disappearance of the superstructure reflections in the x-ray diffraction patterns at high temperature, the phase transition appears to be of the order–disorder type and one can conclude that the electron density around the various yttrium sites (including Y1 and Y3) in the low-temperature (LT) structure must become equal. This means that during the phase transition some mass transport occurs between neighbouring sites on the diamond-like yttrium sublattice ($\text{Y–Y} = 3.2 \text{ \AA}$). Although no structure refinement at high temperature has been performed yet, it is likely that the yttrium sites in the disordered C15-type structure have about 15% defects which are distributed randomly. Another question to be answered is that of the order of the phase transition. Since the space group relation of the HT phase ($Fd\bar{3}m$, No 227) is a minimal nonisomorphic supergroup of the LT phase ($F\bar{4}3m$, No 216), a second-order transition would be allowed. An example for the change of the intensity for the (511, 333) superstructure line of TbNi_2 with temperature is shown in figure 8. The monotonic decrease of this intensity points to a second-order phase transition in TbNi_2 . However, a closer inspection of the high-temperature x-ray data on YNi_2 shows that at least in this case a discontinuous vanishing of this line intensity exists and a first-order character is likely in view of the rather abrupt change in resistivity and thermal expansion especially in the Y, Sm, and Gd compounds.

4. Summary

The results of the present investigations can be summarized as follows.

(i) The RNi_2 compounds with $R = Y, Sm, Gd$ and Tb can be prepared as single-phase samples $R_{1-x}Ni_2$ with x around 0.05 in a superstructure of the cubic Laves phase (space group: $F\bar{4}3m$).

(ii) The reason for which these compounds can be synthesized as single-phase samples at room temperature and ambient pressure in the superstructure but not in the cubic Laves phase is related to insufficient space filling in the cubic Laves phase.

(iii) These RNi_2 compounds show temperature-induced and at least for YNi_2 also pressure-induced phase transitions. The structure above the transition temperature and above 27 GPa for YNi_2 is the cubic Laves phase, however with disordered vacancies at the Y sites.

(iv) The fact that the cubic Laves phase can be stabilized under pressure at room temperature supports the space-filling arguments.

(v) Future pressure experiments on RCu_2 compounds are planned in order to check whether the orthorhombic structure can be transferred into the cubic Laves phase under pressure at room temperature.

Acknowledgments

We would like to thank J Otto for his cooperation and for taking care of the beamline in HASYLAB.

This work was supported by the Austrian 'Fond zur Förderung der wissenschaftlichen Forschung' project number P11581-PHY, the French 'Ministère des Affaires Etrangères' APAPE No 96036/A36, and the Swiss National Science Foundation.

References

- [1] Iandelli A and Palenzona A 1979 *Handbook on the Physics and Chemistry of Rare Earths* vol 2, ed K A Gschneidner Jr and L Eyring (Amsterdam: North-Holland) p 1
- [2] Beaudry B J, Haegling J F and Daane A H 1960 *Acta Crystallogr.* **13** 743
- [3] Paul-Boncour V, Lartigue C, Percheron-Guégan A, Achard J C and Pannetier J 1988 *J. Less-Common Met.* **143** 301
- [4] Paul-Boncour V, Percheron-Guégan A, Escorne M, Mauger A and Achard J C 1989 *Z. Phys. Chem.* **163** 263
- [5] Deutz A F, Helmholtz R B, Moleman A C, de Mooij D B and Buschow K H J 1989 *J. Less-Common Met.* **153** 259
- [6] Latroche M, Paul-Boncour V, Percheron-Guégan A and Achard J C 1990 *J. Less-Common Met.* **161** L27
- [7] Latroche M, Paul-Boncour V and Percheron-Guégan A 1993 *Z. Phys. Chem.* **179** 261
- [8] Fournier J M and Gratz E 1993 *Handbook on the Physics and Chemistry of Rare Earths* vol 17, ed K A Gschneidner Jr, L Eyring, G H Lander and G R Choppin (Amsterdam: North-Holland) p 409
- [9] Slebarski A 1988 *J. Less-Common Met.* **141** L1
- [10] Gratz E, Bauer E, Resel R, Pöllinger S, Mantler M and Nowotny H 1991 *Eur. J. Solid State Inorg. Chem.* **28** 511
- [11] Syassen K and Holzapfel W B 1975 *Europhys. Conf. Abstr.* **1A** 75
- [12] Forman R A, Piermarini G J, Barnett J D and Block S 1972 *Science* **176** 284
- [13] Mao H K 1989 *Simple Molecular Systems at Very High Density* ed A Polian, P Loubeyre and N Boccara (New York: Plenum) p 221
- [14] Blatt F L 1968 *Physics of Electronic Conduction in Solids* (New York: McGraw-Hill)
- [15] Burzo E, Gratz E and Pop V 1993 *J. Magn. Magn. Mater.* **123** 159